Metal-ligand delocalization and spin density in the CuCl2 and [CuCl4]2− molecules: Some insights from wave function theory

Emmanuel Giner and Celestino Angeli

Citation: The Journal of Chemical Physics **143**, 124305 (2015); doi: 10.1063/1.4931639
View online: http://dx.doi.org/10.1063/1.4931639
View Table of Contents: http://scitation.aip.org/content/aip/journal/jcp/143/12?ver=pdfcov
Published by the AIP Publishing

Metal-ligand delocalization and spin density in the $CuCl_2$ and $[CuCl_4]^{2-}$ molecules: Some insights from wave function theory

Emmanuel Giner[a] and Celestino Angeli[b]
Dipartimento di Scienze Chimiche e Famaceutiche, Universita di Ferrara, Via Fossato di Mortara 17, I-44121 Ferrara, Italy

(Received 22 June 2015; accepted 11 September 2015; published online 28 September 2015)

The aim of this paper is to unravel the physical phenomena involved in the calculation of the spin density of the $CuCl_2$ and $[CuCl_4]^{2-}$ systems using wave function methods. Various types of wave functions are used here, both variational and perturbative, to analyse the effects impacting the spin density. It is found that the spin density on the chlorine ligands strongly depends on the mixing between two types of valence bond structures. It is demonstrated that the main difficulties found in most of the previous studies based on wave function methods come from the fact that each valence bond structure requires a different set of molecular orbitals and that using a unique set of molecular orbitals in a variational procedure leads to the removal of one of them from the wave function. Starting from these results, a method to compute the spin density at a reasonable computational cost is proposed. © *2015 AIP Publishing LLC.* [http://dx.doi.org/10.1063/1.4931639]

I. INTRODUCTION

Molecules containing open shell transition metals are challenging systems for the modern computational chemistry. Nowadays, the two most popular computational models are Density Functional Theory (DFT) and Wave Function Theory (WFT) and none of these approaches are able to give a definitive answer to the general problem of the electronic correlation, especially when transition metals are involved. The main difficulties in such systems arise from the requirement to have a balanced description of two key different physical effects: the strong electronic correlation in the highly polarisable $3d$ shell and the delocalization of the electrons between the metals and the ligands. These two effects are known to be highly connected, since the delocalization of the electrons between the metals and the surrounding ligands creates different electrostatic situations, to which the $3d$ shell and the ligand's lone pairs are known to be very sensitive. In open shell systems, the delocalization of the unpaired electrons can be formally quantified by the spin density (SD). Experimentally, this quantity can be determined through several techniques, such as the nuclear magnetic resonance (NMR),[1] polarized neutron diffraction (PND) coupled with maximum entropy,[2] or electron paramagnetic resonance (EPR) spectroscopy.[3] From a theoretical point of view, the SD distribution among the atoms of a system can reveal several physical phenomena, such as the delocalization of the unpaired electrons, the spin polarization, or the degree of ionicity of a metal-ligand bond. The ability of a given computational approach to reproduce correctly the main trends of the SD is crucial as it strongly impacts the calculation of various quantities. Concerning the magnetic coupling in Cu(II) binuclear complexes, for instance, the SD on the metal atoms is strongly related to the level of delocalization of the magnetic orbitals on the surrounding ligands. This metal-ligand delocalization has been intensively studied for a long time,[4–11] and it has been shown that its correct determination is compulsory to reproduce the experimental values of the spin coupling constant. The importance of the delocalization of the magnetic orbitals to compute the spin coupling using perturbation theory has been addressed by several works,[11–13] both using the n-electron valence perturbation theory (NEVPT2[14–16]) and the complete active space second order perturbation theory (CASPT2[17]). Concerning the metal-ligand delocalization itself, it has been shown in Ref. 8 that the magnetic orbitals obtained at various levels of calculation (mean-field, large configuration interaction expansions, and DFT) in Cu(II) binuclear complexes exhibit qualitative different delocalization on the surrounding ligands. In Refs. 8 and 10, the authors have highlighted the fact that a notable metal-ligand delocalization appears when treating together two particular classes of excitations, namely, the $1h$ and $2h1p$ in the difference dedicated configuration interaction (CI) language,[18] on top of the complete active space (CAS). In such work, the $1h$ were identified as ligand to metal charge transfer (LMCT), and it has been shown that at difference dedicated CI (DDCI) level their coefficient considerably improved with respect to the CAS+S level. For the singlet state, this was attributed to the interaction of the LMCT configuration with the ionic forms of metal-metal charge transfer nature present in the minimal CAS(2,2) description of the singlet. For the triplet state, where the ionic components are vanishing, the importance of the LMCT determinants was ascribed to the interaction with the $2h1p$ determinants which lower the effective energy of the LMCT configuration, giving a ferromagnetic contribution to the spin coupling. Nevertheless, all these mechanisms are intrinsically linked to the presence of two magnetic centers, whether for the metal-metal ionic forms or of the polarization of the hole from where the charge transfer has been created. Other works by Broer *et al.*[5,9] have highlighted the role

[a]Electronic mail: gnrmnl@unife.it
[b]Electronic mail: anc@unife.it

of the LMCT states in the metal-ligand delocalization using the non-orthogonal CI (NOCI) method. A notable difference of such approach with respect to the considerations reported in Ref. 10 relies in the interpretation of the mechanism of metal-ligand delocalization: starting from self consistent field (SCF) orbitals, the rising of the LMCT coefficient has been attributed in Ref. 10 to the dynamical correlation through high order effects, whereas Broer *et al.* have pointed out the importance of the orbital relaxation of the LMCT states. Another practical impact of the correct/incorrect determination of the SD concerns the treatment of the spin orbit (**SO**) operator. This was highlighted in the flourishing field of EPR spectroscopy, where lot of effort has been devoted to reproduce the experimental EPR spectrum through the mapping of the spin Hamiltonian thanks to *ab initio* calculations. In this field, the SD on the metal ions impacts drastically the calculation of the **g** tensor, because of its importance on the **SO** matrix elements, as it has been highlighted in Refs. 19–21, for instance.

The purpose of this paper is to study the main mechanisms affecting the determination of the spin density for two mono nuclear inorganic compounds, namely, $CuCl_2$ and $[CuCl_4]^{2-}$, within the WFT scheme. The paper is built as follows. The first part contains a summary of the previous works in which the calculation of the SD for $CuCl_2$ and $[CuCl_4]^{2-}$ has been investigated. Next, the attention is dedicated to $CuCl_2$ as a model system, with the aim to reveal the key physical effects and the issues one has to face studying copper complexes with WFT. Calculations in a modest basis set (6-31G[22,23]) are carried out up to near full configuration interaction (FCI) to obtain reference values for the SD. The analysis of this "near FCI" wave function and of the relevant Hamiltonian matrix elements provides useful information to explain the key physical effects involved in the qualitative changes of the SD passing from the mean-field to the "near-FCI" wave functions. Then, the importance of the MO set used in the context of correlated methods is investigated. It is shown that the MOs have a drastic impact on the computed values of the SD and that this is the main source of the observed computational issues for this molecule. Thanks to this understanding, a minimal CI space is proposed to obtain accurate SD at a reasonable computational cost. This minimal space is subsequently used to investigate the effect of the basis set for the $CuCl_2$ system and then applied to $[CuCl_4]^{2-}$ where experimental SD is available.[24,25] Finally, the main results of the present work are summarized in the conclusion.

II. A SUMMARY OF THE PREVIOUS WORKS RELATED TO THE SPIN DENSITY IN $CuCl_2$ AND $[CuCl_4]^{2-}$

The SD of the $^2\Pi_g$ ground state of $CuCl_2$ has been investigated using WFT and DFT with various functionals by Ramírez-Solís *et al.*,[26] and Caffarel *et al.*[27] The main results for the SD on the copper atom using the Mulliken population analysis (MPA)[28] are shown in Table I.

TABLE I. Summary of the SD values on the copper atom obtained with different DFT and WFT approaches for the $^2\Pi_g$ ground state of $CuCl_2$ using the Mulliken population analysis.

Method	$^2\Pi_g$ SD (Cu)
BLYP[a]	0.43
PBE96[a]	0.43
HCTH407[a]	0.42
TPSS[a]	0.41
M06-2X[a]	0.65
B3LYP[a]	0.57
B97-2[a]	0.54
CASSCF(21-15)[a]	0.94
ROHF (6-31g)[b]	0.94
CIPSI (6-31g)[b]	0.87

[a]Results obtained in Ref. 26.
[b]Results obtained in Ref. 27.

At the DFT level, the unpaired electron is strongly delocalized on the chlorine ligands, with the SD on the copper atom having values ranging from 0.41 to 0.65 with the TPSS[29] and M06-2X[30] functionals, respectively. These differences can be related to the percentage of Hartree-Fock exchange (E_X^{HF}) present in the various functionals. The sensitivity of the global shape of the SD to the percentage of E_X^{HF} in the B3LYP[31–33] functional has been investigated in more detail in Ref. 27. From this study, it appears that the smaller the percentage of E_X^{HF}, the bigger the delocalization of the singly occupied molecular orbital (SOMO) on the chlorine ligands. A similar behaviour has been also reported for other Cu(II) complexes.[34–36] Using a WFT strategy at the mean-field level, both restricted open shell Hartree-Fock (ROHF) and complete active space self consistent field (CASSCF), the unpaired electron is essentially centered on the copper atom. A near-FCI wave function in a modest basis set (6-31G) can be computed thanks to the configuration interaction with perturbative selection done iteratively (CIPSI).[37,38] At this level, an intermediate situation is found with a SD of 0.87 on the copper atom. More precisely, Caffarel *et al.*[27] had to enlarge the CI space up to a million Slater determinants in the CIPSI algorithm to reach the convergence of the global shape of the SD, suggesting that the electronic correlation plays an important role in the delocalization of the unpaired electron. From these results, it clearly appears that the SDs obtained from WFT and DFT are qualitatively different. Unfortunately, there are no experimental data available for the SD of this molecule, which prevents us to know what is the best computational approach in this case.

Considering now the SD of the $^2B_{1g}$ ground state of $[CuCl_4]^{2-}$ in its tetragonal structure, experimental data are available[24,25] and a value of 0.62 ± 0.02 electrons on the copper atoms has been found. Szilagyi *et al.*[34] have performed a calibration of the gradient corrected (GGA) BP86 functional[39,40] to match the experimental ground state SD. The only parameter was the amount of E_X^{HF}, which was found to be optimal at 38%, roughly twice the percentage used in the B3LYP functional. It should be noticed that with such a modified BP86 functional, the calculated excitation energies for the LMCT and ligand field (LF) transitions were also substantially improved with respect to standard BP86, B3LYP, or BHandHLYP functionals. In Refs. 36 and 41, the optimization of the E_X^{HF} percentage in various hybrid functionals was also reported for this molecule, as a model for copper proteins in the context of the simulation of EPR spectra. Using WFT in the same context, Pierloot *et al.* performed multireference calculations both variational

and by perturbation.[20,21] In the first study,[20] the **g** tensor was calculated using a CASPT2 with a CASSCF zeroth order wave function. The **g** tensor was found to be in poor agreement with the experimental value. This effect was attributed to an overestimation of the SD on the copper atom by the zeroth order CASSCF wave function, 0.84 electrons instead of the 0.62 ± 0.02 value experimentally measured. In the second part of the study,[21] a multistate CASPT2 (MS-CASPT2) approach was applied. In the present context, the main results of this study are that the mixing of the CASSCF ground state with a LMCT excited state (more than 6 eV above the ground state) considerably improves the calculation of the **g** tensor. More precisely, by allowing the perturbation correction to bridge the interaction between these two CASSCF eigenstates (Perturbation Modified CASPT2, PMCASPT2), one recovers the experimental value of the SD on the copper atom, which is known to be crucial for the **L** and **SO** matrix elements. The impact of the SD on the calculation of the **g** tensor through the various **L** and **SO** matrix elements has been also observed on other Cu(II) complexes, such as $[Cu(NH_3)_4]^{2+}$ by Neese[19] and Pierloot *et al.*[20,21]

From the analysis of these selected works, concerning the determination of the SD on the two molecules we are interested in, one can extract two major trends. At the DFT level, this quantity depends strongly on the percentage of E_X^{HF}, which seems to be too low in the B3LYP functional, for instance. From the WFT perspective, the mean-field approach, both single and multireference, overestimates the SD on the metal atom, exaggerating the ionic character of the Cu–Cl bond. The effect of the electronic correlation is then crucial to recover the correct SD and seems to have to be treated in a rather sophisticated way, given that the convergence of this property with respect to the quality of the wave function is very slow.

III. A CASE STUDY: THE $CuCl_2$ MOLECULE

The present section is dedicated to the detailed analysis of the various physical effects which have to be included in the calculation of the SD in $CuCl_2$ using wave function approaches.

The copper atom is at the origin of the reference frame, while the two chlorine atoms are placed along the z axis at ±3.9 Å (that is, a Cu–Cl distance close to the experimental value of 3.85 Å[42]). In order to focus on the spatial distribution of the spin density, we chose the following definition for the integrated spin density:

$$\Delta\rho(z_i) = \frac{1}{\Delta z}\int_{-\infty}^{+\infty} dy \int_{-\infty}^{+\infty} dx \int_{z_i-\frac{\Delta z}{2}}^{z_i+\frac{\Delta z}{2}} dz \left[\rho_\alpha(\mathbf{r}) - \rho_\beta(\mathbf{r})\right], \tag{1}$$

where $\rho_\alpha(\mathbf{r})$ and $\rho_\beta(\mathbf{r})$ are the α and β spin densities, z_i is a regular grid in z with $z_{i+1} - z_i = \Delta z$, and $\Delta z = 0.1$ a.u. In order to get reference values for $\Delta\rho(z)$, the same road reported in Ref. 27 is followed, performing a near-FCI calculation in a modest basis set (6-31G). To reduce the size of the FCI space, the neon and argon cores for the chlorine and copper atoms, respectively, are kept frozen. This results in an active space of 25 electrons in the remaining 36 orbitals, leading to a total FCI space of about 10^{18} determinants. Of course, the diagonalization of such CI matrix cannot be achieved by standard CI techniques. To tackle the problem, the CIPSI algorithm[37,38] has been used, as detailed in the following paragraph. The analysis of the converged CIPSI wave function is performed in terms of Valence Bond (VB) structures and the impact on $\Delta\rho(z)$ of the various classes of excitations is discussed. Finally, a detailed analysis of the most important Hamiltonian matrix elements in the CIPSI space is discussed and the effect of the size consistency is investigated through the use of the configuration interaction with single and double excitations (CISD) and also with the CISD self consistent and size consistent approach (CISD(SC)^2).[43–45]

A. Reference value for the spin density with CIPSI calculations

In the CIPSI algorithm, the configurations are selected iteratively by estimating their contribution to the energy at second order in perturbation theory (PT) or to the wave function at first order, allowing one to keep only the determinants having a significant impact on the energy and/or on the wave function. The concept of a selected CI algorithm with a selection guided by PT is not new in computational chemistry[37,38,46–49] and the CIPSI algorithm is one of the pioneering approaches in this field. It has been used and analyzed intensively in the past decades,[38,50–53] and also recently reintroduced in the context of fixed node diffusion Monte Carlo (FN-DMC)[54–56] and in other contexts.[57] In detail, one starts the CIPSI procedure with a given reference wave function $|\psi_{\text{ref}}\rangle$ expressed as a linear combination of N_{ref} Slater determinants spanning what is called the $\mathcal{S}$ space,

$$|\psi_{\text{ref}}\rangle = \sum_{\text{I}\in\mathcal{S}} c_{\text{I}}|\text{I}\rangle, \tag{2}$$

where the coefficients c_{I} are obtained by the minimization of the variational energy E_{ref} of $|\psi_{\text{ref}}\rangle$,

$$E_{\text{ref}} = \min_{\{c_{\text{I}}\}} \frac{\langle\psi_{\text{ref}}|H|\psi_{\text{ref}}\rangle}{\langle\psi_{\text{ref}}|\psi_{\text{ref}}\rangle}. \tag{3}$$

Considering a given determinant $|\mu\rangle$ not belonging to the $\mathcal{S}$ space, its coefficient at first order (using here the Epstein Nesbet zeroth order Hamiltonian[58,59]) is given by

$$\begin{aligned} c_\mu^{(1)} &= \frac{\langle\mu|H|\psi_{\text{ref}}\rangle}{E_{\text{ref}} - \langle\mu|H|\mu\rangle} \\ &= \sum_{|\text{I}\rangle\in\mathcal{S}} c_{\text{I}} \frac{\langle\mu|H|\text{I}\rangle}{E_{\text{ref}} - \langle\mu|H|\mu\rangle}. \end{aligned}$$

The contribution of $|\mu\rangle$ to the energy at second order in PT is

$$\begin{aligned} e_\mu^{(2)} &= c_\mu^{(1)}\langle\psi_{\text{ref}}|H|\mu\rangle \\ &= \frac{|\langle\mu|H|\psi_{\text{ref}}\rangle|^2}{E_{\text{ref}} - \langle\mu|H|\mu\rangle}. \end{aligned}$$

An iteration of the CIPSI algorithm consists in selecting the $|\mu\rangle$ determinants with a contribution $e_\mu^{(2)}$ greater than a given threshold η. The reference space $\mathcal{S}$ is then augmented by the selected $|\mu\rangle$ and the coefficients in Eq. (2) are reoptimized to obtain a new reference wave function. This procedure is iterated lowering the selection threshold η. This selection scheme

is hereafter referred to as the "E-selection." Other selection schemes are possible, see, for instance, the "aimed selection."[52] In the present study, the calculations are stopped when the size of the reference space $\mathcal{S}$ reaches a given number of determinants fixed in the beginning of the procedure. The convergence of a given quantity (as, for instance, the variational energy or $\Delta\rho(z)$) is studied as a function of the number of determinants present in the $\mathcal{S}$ space. It should be emphasized that the CIPSI selection scheme is not based on an *a priori* selection criterion expressed according to the degree of excitation with respect to a given reference space, as it is usually done in truncated CI calculations. The CIPSI algorithm, thanks to the iterative PT strategy, realizes an adaptive selection.

In order to study the importance of the selection criterion, another version of CIPSI has been implemented based on the work of Angeli and Cimiraglia.[60] The key idea is a selection scheme based on a one body property of interest. In practice, the selection is done by the estimation, at the first order in PT, of the contribution of a $|\mu\rangle$ determinant to the expectation value of a given one body operator $\hat{O}_1$. This approach has shown to improve the convergence of the target one body property for selected case studies. With respect to the original proposal, here a part of the second order contribution is also considered and the contribution of the determinant $|\mu\rangle$ to the expectation value of $\hat{O}_1$ is taken as

$$o_\mu^{(2)} = c_\mu^{(1)} \left(2\langle\psi_{\text{ref}}|\hat{O}_1|\mu\rangle + c_\mu^{(1)}\langle\mu|\hat{O}_1|\mu\rangle\right). \tag{4}$$

In the present context, the one body operator used is of course the spin density $\Delta\rho(z)$, and given that the $\Delta\rho(z)$ vanishes at the nucleus of the copper atom (i.e., at $z = 0$ Å), $\Delta\rho(z)$ is computed at $z = 3.9$ Å, that is, near one chlorine atom. The contribution of a given determinant $|\mu\rangle$ to $\Delta\rho(z)$ at the nucleus of one chlorine atom is

$$\Delta\rho_\mu^{(2)} = c_\mu^{(1)} \left(2\langle\psi_{\text{ref}}|\Delta\rho(z)|\mu\rangle + c_\mu^{(1)}\langle\mu|\Delta\rho(z)|\mu\rangle\right), \quad z = 3.9 \text{ Å}. \tag{5}$$

In this version of the CIPSI algorithm, a determinant $|\mu\rangle$ is selected if the absolute value of $\Delta\rho_\mu^{(2)}$ is greater than a certain threshold η. This will be referred to as the "$\Delta\rho$ selection." In the following paragraph, the numerical results of the CIPSI calculations are presented. The molecular orbitals (both occupied and virtual) are taken from a standard ROHF calculation done using the GAMESS(US) program[61] and all CI and perturbation calculations are done with the *Quantum Package* program,[62] an open source post Hartree-Fock program developed recently by Scemama, Applencourt, Caffarel, and Giner.

The convergence of the variational energy of the $^2\Pi_g$ ground state computed using the $\Delta\rho$-selection and E-selection, as well as the estimated FCI energy extracted from the data of Caffarel *et al.* is reported in Figure 1. This figure shows that, as expected, the variational energy converges faster for the E-selection than for the $\Delta\rho$-selection. Nevertheless, at large number of determinants, the energies for both selection schemes are quite close to the estimated FCI value,[27] indicating that the associated wave functions are of very high quality. It should be stressed here that reaching a near-FCI energy with a variational method is remarkable in a FCI space containing approximately 10^{18} determinants. The

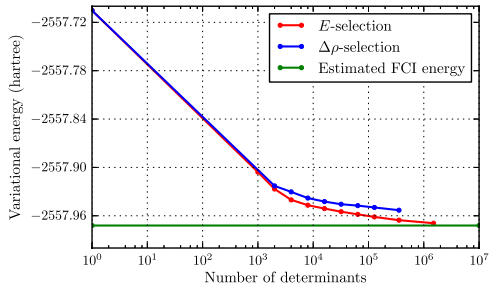

FIG. 1. Convergence of the variational energy (hartree) for the CIPSI wave function using the $\Delta\rho$-selection and E-selection compared to the converged CIPSI energy of Caffarel *et al.*,[27] as a function of the number of determinants. ROHF molecular orbitals are used.

values of $\Delta\rho(z)$ at $z = 3.9$ Å for the various CIPSI wave functions are presented in Figure 2, from which it appears that the rising of the SD near the chlorine atoms is faster with the $\Delta\rho$-selection. Nevertheless, the values obtained at large numbers of determinants for both selection schemes are comparable, indicating that a value of $\Delta\rho(z) = 0.046$ at $z = 3.9$ Å is a good approximation of the FCI value. It is worth noticing that reaching the convergence for the SD requires approximatively 10^6 determinants, even using the $\Delta\rho$-selection, which means that, in the present case, the selection criterion of the CIPSI algorithm does not have a major impact on the convergence speed of this one body property. It should be emphasized that the slow convergence of this one body property with the size of the variational space is quite remarkable, highlighting the difficulty for this system of determining $\Delta\rho(z)$ using WFT.

In order to get a more global picture of the shape of the SD at different levels of calculations, we report in Figure 3 the plot of $\Delta\rho(z)$ as a function of z computed with three different wave functions using the 6-31G basis set: ROHF, CASSCF(21,15), and the CIPSI wave functions containing 1.5×10^6 determinants selected with the $\Delta\rho$-selection. Here, the CASSF is composed of the 3d, 4s, and 4p shells of the copper atom, together with the 3p shell of each chlorine atom, which leads to a complete active space of 21 electrons in 15 orbitals, whose size is approximatively around 40 000 determinants. From this picture, it appears clearly that there is a qualitative change of the SD between the mean-field wave functions (both single and multireference) and the near-FCI wave function. The CIPSI wave function gives a notable delocalization of the unpaired electron on the chlorine ligands, while the

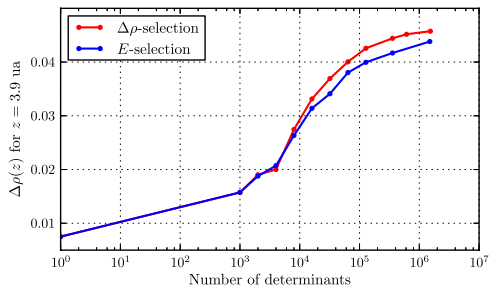

FIG. 2. Convergence of the value of $\Delta\rho(z)$ for $z = 3.9$ Å calculated from CIPSI wave functions obtained using the $\Delta\rho$-selection and E-selections as a function of the number of determinants. ROHF molecular orbitals are used.

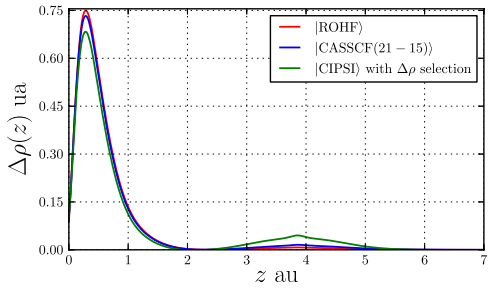

FIG. 3. $\Delta\rho(z)$ for the ROHF, CASSCF(21,15), and CIPSI wave functions containing 1.5×10^6 determinants selected with the $\Delta\rho$-selection.

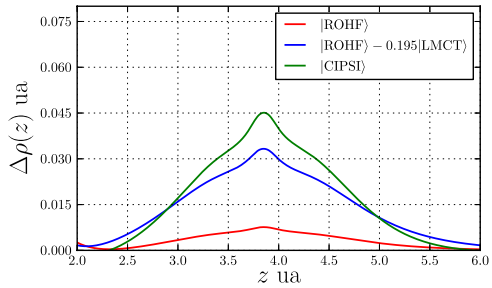

FIG. 4. $\Delta\rho(z)$ around one chlorine atom for the normalized wave function containing only the ROHF and LMCT determinants with their relative coefficients taken from the CIPSI wave function. Comparison with the ROHF and CIPSI values.

mean-field wave functions mainly localize the unpaired electron on the copper atom.

B. Qualitative analysis of the CIPSI wave function

To understand how the delocalization of the unpaired electron occurs at the CIPSI level, a qualitative analysis of the wave function is proposed in this paragraph. This analysis is reported here for a CIPSI wave function containing 1.5 $\times 10^6$ determinants selected with the $\Delta\rho$-selection, indicated as |CIPSI⟩. In this wave function, the determinant having the largest weight after the ROHF determinant is a single excitation of a β electron from a b_{2g} orbital (referred here to as the $b_{2g}(p_x)$ orbital) to the SOMO, also belonging to the b_{2g} irreducible representation. The $b_{2g}(p_x)$ orbital is essentially composed of the out of phase combination of the chlorine atom $3p_x$ orbitals and the SOMO is dominated by the copper $3d_{xz}$ atomic orbital. Therefore, the single excitation from the $b_{2g}(p_x)$ to the SOMO can be thought as a charge transfer from the ligand to the metal and it will indicated here as the LMCT determinant (|LMCT⟩),

$$|\text{LMCT}\rangle \equiv a^{\dagger}_{\beta\ \text{SOMO}} a_{\beta\ b_{2g}(p_x)} |\text{ROHF}\rangle. \tag{6}$$

The two main configurations of the CIPSI wave function can be analyzed in terms of VB structures. The ROHF determinant represents the $Cl^-Cu^{2+}Cl^-$ VB structure where the Cu^{2+} cation and Cl^- anions are, respectively, in the $[Ar]3d^9$ and the $[Ne]3s^23p^6$ electronic configurations. On the other hand, the |LMCT⟩ configuration represents the resonance of the two Cl^-Cu^+Cl and $ClCu^+Cl^-$ VB structures, in which the Cu^+ cation is in the $3d^{10}$ electronic configuration.

In order to emphasize the role of the |LMCT⟩ configuration, Figure 4 reports the shape of $\Delta\rho(z)$ (closed to one chlorine atom) computed with the normalized wave function containing only the ROHF and LMCT determinants with their relative coefficients taken from the CIPSI wave function.

From this figure, it appears that the main delocalization effect of the unpaired electron from the Cu atom to the chlorine ones occurring at the CIPSI level can be taken into account using only the two dominant configurations (|ROHF⟩ and |LMCT⟩) if one knows their relative coefficients. In the CIPSI wave function, the amplitude of the |LMCT⟩ configuration (that is, the ratio between the coefficient of the |LMCT⟩ and the coefficient of the |ROHF⟩) is −0.195. The fact that this single excitation has such an important coefficient is unusual at least for two reasons. First, its energy is 11.15 eV higher than the ROHF energy, which means that no near degeneracy effects can explain its importance in the wave function. Second, the |LMCT⟩ configuration, being a single excitation, does not interact with the ROHF determinant (which is the dominant determinant in the CIPSI wave function) because of the Brillouin theorem.[63,64] Therefore, one can wonder how such an unfavoured determinant ends up to be the second most important determinant after |ROHF⟩. The next paragraph is dedicated to answer this question.

C. The origin of the importance of the |LMCT⟩ configuration

From single reference perturbation theory (SRPT), the first non-vanishing contribution to the coefficient of the |LMCT⟩ configuration appears at second order for the wave function, due to its interaction with the double excitations, suggesting that the double excitations play a major role for the inclusion of the |LMCT⟩ configuration. To investigate this effect, a CISD calculation has been performed and the shape of $\Delta\rho(z)$ obtained at this level is reported in Figure 5. From this figure, it appears that the CISD wave function does not reproduce correctly the SD. Of course, it is well known that CISD is the archetype of truncated CI presenting strong size consistency errors and such errors have large impact on the |LMCT⟩ configuration whose amplitude is −0.07 in the CISD wave function, far from −0.195, the value obtained in the near-FCI wave function.

To study the impact of the size consistency error in the determination of the correct SD, the CISD(SC)^2 approach has been chosen, rather than the coupled cluster with single and

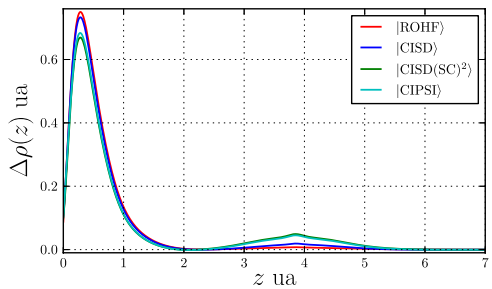

FIG. 5. $\Delta\rho(z)$ calculated with the CISD and CISD(SC)^2 wave functions, compared with the CIPSI and ROHF $\Delta\rho(z)$.

double (CCSD) or the quadratic CISD[65] (QCISD), which are also size consistent methods. This choice has been motivated by the fact that CISD(SC)^2 suppresses exactly and only the disconnected terms present in the CISD calculation, which are known to be the root of size consistency errors,[66] whereas CCSD and QCISD introduce also various correlation effects (such as connected terms), thus overpassing the strict boundaries of the size consistency problem. The global shape of $\Delta\rho(z)$ calculated with the CISD(SC)^2 wave function is also shown in Figure 5 and it is found to be very close to the near-FCI spin density. Once more, there is a correlation between the quality of the SD obtained with a given wave function and the amplitude of the |LMCT⟩ determinant. In the CISD(SC)^2 wave function its value is −0.23, very close to the best value, −0.195. The only difference between the CISD and CISD(SC)^2 is the disconnected terms present in the CISD eigenvalue equation, which are suppressed in the CISD(SC)^2 eigenvalue equation by taking into account (through a dressed Hamiltonian) the possible repeatability of the double excitation operations that would generate triple and quadruple excitations.[43,67] This mechanism can also explain why the CIPSI algorithm manages to give such an importance to the |LMCT⟩ configuration, even if it remains a truncated CI approach submitted to size consistency errors: the triple and quadruple excitations, present in the CIPSI wave function, kill a huge part of the disconnected terms, allowing the double excitations to have correct coefficients and then the |LMCT⟩ coefficient to rise properly. This suggests that the physics giving the correct coefficient of the |LMCT⟩ determinant is within the double excitations, once the size consistency error has been eliminated.

Among the double excitations, those who are single excitations on top of the |LMCT⟩ determinants are found to strongly interact with it. In order to study the impact of these double excitations using a semi quantitative model, a second order state specific intermediate Hamiltonian[68,69] has been built. The model space is spanned by the ROHF determinant, the intermediate model space is the |LMCT⟩ determinant, and the outer space is built with all single excitations on top of the |LMCT⟩ determinant (many of them are double excitations with respect to the ROHF determinant). It should be pointed out that in the present case, as there are no interactions between the determinants in the model space and intermediate space, such an approach is free from size consistency errors as it can be shown in Ref. 70. For the sake of clarity, the ROHF energy has been subtracted on the diagonal. The explicit definition of the intermediate Hamiltonian matrix elements is

$$
\begin{aligned}
\langle \mathrm{ROHF}|H^{(eff)}|\mathrm{ROHF}\rangle &= \sum_{\mu} \frac{|\langle \mathrm{ROHF}|H|\mu\rangle|^2}{E_{\mathrm{ROHF}} - \langle\mu|H|\mu\rangle}, \\
\langle \mathrm{ROHF}|H^{(eff)}|\mathrm{LMCT}\rangle &= \langle \mathrm{LMCT}|H^{(eff)}|\mathrm{ROHF}\rangle \\
&= \langle \mathrm{ROHF}|H|\mathrm{LMCT}\rangle + \sum_{\mu} \frac{\langle \mathrm{ROHF}|H|\mu\rangle\langle\mu|H|\mathrm{LMCT}\rangle}{E_{\mathrm{ROHF}} - \langle\mu|H|\mu\rangle}, \\
\langle \mathrm{LMCT}|H^{(eff)}|\mathrm{LMCT}\rangle &= \langle \mathrm{LMCT}|H|\mathrm{LMCT}\rangle - \langle \mathrm{ROHF}|H|\mathrm{ROHF}\rangle + \sum_{\mu} \frac{|\langle \mathrm{LMCT}|H|\mu\rangle|^2}{E_{\mathrm{ROHF}} - \langle\mu|H|\mu\rangle},
\end{aligned}
\tag{7}
$$

where the $|\mu\rangle$ determinants are all single excitations on top of the |LMCT⟩ determinant, excluding, of course, the ROHF determinant. The explicit values of the "naked" Hamiltonian (that is, without the perturbative dressing from the $|\mu\rangle$) and of the intermediate Hamiltonian corrected to second order are reported in Figure 6 (in eV).

$$
H = \begin{array}{c} \\ \langle \mathrm{ROHF}| \\ \langle \mathrm{LMCT}| \end{array}
\begin{array}{c} \begin{array}{cc} |\mathrm{ROHF}\rangle & |\mathrm{LMCT}\rangle \end{array} \\ \begin{pmatrix} 0.00 & 0.00 \\ 0.00 & 11.15 \end{pmatrix} \end{array}
$$

$$
H^{(eff)} = \begin{array}{c} \\ \langle \mathrm{ROHF}| \\ \langle \mathrm{LMCT}| \end{array}
\begin{array}{c} \begin{array}{cc} |\mathrm{ROHF}\rangle & |\mathrm{LMCT}\rangle \end{array} \\ \begin{pmatrix} -0.16 & 1.24 \\ 1.24 & 1.50 \end{pmatrix} \end{array}
$$

FIG. 6. Exact Hamiltonian (H, up) projected on the |ROHF⟩ and |LMCT⟩ configurations and intermediate Hamiltonian ($H^{(eff)}$, down) projected on the same space taking into account at second order the effect of the $|\mu\rangle$ determinants that are single excitations on top of the |LMCT⟩ configuration. Values in eV.

Several effects can be observed from these Hamiltonians. The first one is that, thanks to the $|\mu\rangle$ determinants, an effective interaction of about 1.24 eV is observed between the ROHF and the LMCT determinants, allowing for the mixing of these two configurations in the ground state of $CuCl_2$. Furthermore, the differential effect of the $|\mu\rangle$ on the effective energies of |ROHF⟩ and |LMCT⟩ is huge because the energy difference passes from 11.15 eV without the dressing to 1.66 eV once the perturbation is included, suggesting that the $|\mu\rangle$ should not be treated by perturbation. To justify this assumption, the $H^{(eff)}$ has been diagonalized: in its lowest eigenstate, the |LMCT⟩ configuration has an amplitude of about −0.5, which is more than twice the amplitude of the same determinant in the near-FCI wave function. This result further confirms that the effect of the single excitations on top of the |LMCT⟩ determinant cannot be treated by a perturbation approach.

It is worth noticing that most of the $|\mu\rangle$ determinants are double excitations with respect to the ROHF configuration, which means that they should introduce some correlation effects. Nevertheless, with respect to the |LMCT⟩

configuration they are single excitations suggesting that their role is to relax the orbitals for the |LMCT⟩ determinant. Given that the $|\mu\rangle$ cause a lowering of the effective energies which are much more important for the |LMCT⟩ than for the ROHF configuration (9.65 eV and 0.16 eV, respectively), the dominant effect is the relaxation of the orbitals of the |LMCT⟩ determinant. Nevertheless, even if the lowering of the effective energy caused by the orbital relaxation is more spectacular than the effective interaction that appears between the |ROHF⟩ and |LMCT⟩ configurations, without the latter the two configurations could not mix in the ground state. Considering a determinant $|\mu\rangle$ which is a single excitation on top of |LMCT⟩ ($|\mu\rangle = a_r^\dagger a_i|\text{LMCT}\rangle$), the contribution to the effective interaction between |ROHF⟩ and |LMCT⟩ is proportional to $(ir, \text{SOMO}b_{2g}(p_x)) \times \langle r|J_{SOMO} - J_{b_{2g}(px)}|i\rangle$, where the integrals are defined as

$$(ij,kl) = \int d\mathbf{r}_1 \int d\mathbf{r}_2\ \phi_i(\mathbf{r}_1)\phi_j(\mathbf{r}_1)\frac{1}{\mathbf{r}_{12}}\phi_k(\mathbf{r}_2)\phi_l(\mathbf{r}_2), \quad (8)$$

$$\langle\phi_i|J_j|\phi_k\rangle = \int d\mathbf{r}_1 \int d\mathbf{r}_2\big(\phi_j(\mathbf{r}_1)\big)^2\frac{1}{\mathbf{r}_{12}}\phi_i(\mathbf{r}_2)\phi_k(\mathbf{r}_2). \quad (9)$$

The contribution of the very same determinant to the effective energy of |LMCT⟩ is proportional to $\langle r|J_{SOMO} - J_{b_{2g}(px)}|i\rangle^2$. In Ref. 6, the authors showed that there is a relation of proportionality between $(ir, \text{SOMO}b_{2g}(p_x))$ and $\langle r|J_{SOMO} - J_{b_{2g}(px)}|i\rangle$, which means that the contribution of $|\mu\rangle$ to the effective energy of |LMCT⟩ is directly proportional to the effective interaction between |ROHF⟩ and |LMCT⟩. In other words, there is a direct relation between the strong orbital relaxation of |LMCT⟩ and the coupling term between |LMCT⟩ and |ROHF⟩. Having such an important impact on the effective parameters of $H^{(eff)}$, the orbital relaxation for the |LMCT⟩ determinant indicates that its optimal orbitals are different from those obtained by the ROHF optimization. Sec. III D is dedicated to the investigation of the role of the used MOs.

D. The role of the molecular orbitals

The request of the orbital relaxation for the LMCT determinant can be easily understood, given that it represents the resonance of two electrostatic situations (ClCu^+Cl^- and $\text{Cl}^-\text{Cu}^+\text{Cl}$) which are markedly different from that represented by the ROHF determinant ($\text{Cl}^-\text{Cu}^{2+}\text{Cl}^-$). The aim of this paragraph is to show that the problem of the correct determination of the delocalization of the unpaired electron comes from the fact that the two important VB structures require different orbitals.

1. Near optimal orbitals for the |LMCT⟩ configuration

The optimal orbitals for the LMCT configuration can be obtained from a general rotation of the canonical orbitals, which at first order reduces to a CI expansion considering the LMCT and all single excitations on top of it,

$$|\text{LMCT}\rangle_{opt} \approx c_{|\text{LMCT}\rangle}|\text{LMCT}\rangle + \sum_{p>q}\sum_{\sigma=\alpha,\beta} c_{pq}^{\sigma} a_\sigma^\dagger\ {}_p a_\sigma\ {}_q|\text{LMCT}\rangle. \quad (10)$$

Of course, one has to exclude the single excitation bringing back to the ROHF determinant. The diagonalization of the CI matrix expressed in this determinant basis gives the optimal coefficients for the $|\text{LMCT}\rangle_{opt}$ wave function. An analysis of the Hamiltonian matrix elements has revealed a number of large interactions (in the range of 4–7 eV) between the LMCT determinant and the determinants in which an electron occupying a $3d$ copper's orbital is excited to copper's d' diffuse virtual orbitals. All these Hamiltonian matrix elements are dominated by bielectronic integrals $\langle\phi_{3d}|J_{3d_{xz}}|\phi_{d'}\rangle$ which give the contribution of the β electron occupying the $3d_{xz}$ copper's orbital in the LMCT configuration to its own Fock operator (see Ref. 71). Of course, other polarization terms involving the chlorine orbitals are also present, but they are less important, suggesting that the dominant effect is the polarization of the $3d$ electrons of the copper atom. To study quantitatively the differences between the natural orbitals of the $|\text{LMCT}\rangle_{opt}$ (indicated hereafter as NO-LMCT) and the ROHF orbitals, the overlap between the two MO sets has been computed obtaining the corresponding orbitals[72] for both MO sets, together with the average value of $\langle x^2\rangle$, $\langle y^2\rangle$, and $\langle z^2\rangle$ for each set of MOs. The five orbitals with the lowest overlap are reported in Table II.

From this table, it clearly appears that the overlaps between the two MO sets are all greater than 0.96, which means that the optimal orbitals for each VB structure are qualitatively equivalent. The main difference between the two MO sets concerns the $3d^{\text{Cu}}_{2z^2-(x^2+y^2)}$ orbital which is more diffuse for the LMCT structure. This can be understood considering that the copper atom passes from Cu^{2+} in the ROHF determinant to Cu^+ in the |LMCT⟩ configuration. The energy difference between the LMCT configuration expressed in the NO-LMCT MO set and the ROHF determinant is 5.6 eV, showing that the orbital relaxation for the LMCT configuration, not completely accounted for at this level, is at least 5.55 eV (the energy difference passes from 11.15 eV to 5.6 eV). On the other hand, the energy of the $\text{Cl}^-\text{Cu}^{2+}\text{Cl}^-$ VB configuration described with the NO-LMCT is 2.20 eV higher than that of the LMCT structure expressed with the same orbitals. This reveals the high sensitivity of the energetic ordering of the VB structures on the MOs. A similar dependency on the molecular orbitals of the relative energies of electronic configurations differing by a charge transfer has been previously observed in different contexts, see, for instance, Refs. 73 and 74. In such works, the target was the calculation of the energy separation of electronic states dominated by two different

TABLE II. Overlap between the corresponding orbitals obtained from the ROHF orbitals and the $|\text{LMCT}\rangle_{opt}$ natural orbitals and the $\langle x^2\rangle$, $\langle y^2\rangle$, and $\langle z^2\rangle$ values (left for ROHF orbitals, right for $|\text{LMCT}\rangle_{opt}$ natural orbitals) for each type of molecular orbital.

Nature of orbital	Overlap	$\langle x^2\rangle$	$\langle y^2\rangle$	$\langle z^2\rangle$
$3d^{\text{Cu}}_{2z^2-(x^2+y^2)}$	0.9620	0.321/0.927	0.294/0.886	0.985/1.93
$3p_z^{\text{Cl}_1} - 3p_z^{\text{Cl}_2}$	0.9981	1.118/1.180	1.192/1.257	11.51/12.0
$3d^{\text{Cu}}_{xz}$	0.9981	0.728/0.738	0.242/0.246	2.970/3.07
$3p_z^{\text{Cl}_1} + 3p_z^{\text{Cl}_2}$	0.9985	0.890/0.845	0.890/0.845	12.89/13.5
$3d^{\text{Cu}}_{xy}$	0.9988	0.202/0.207	0.607/0.623	1.980/2.05

electronic distributions, whereas the present study is focussed on the correct mixing of two electronic structures in the ground state.

It should be stressed that such a mixing in the $CuCl_2$ ground state could be obtained with a unique determinant in which the SOMO will have proper delocalization tails on the chlorine $3p_x$ atomic orbitals. At this point, one can qualitatively understand why the $ClCu^+Cl^-$ and Cl^-Cu^+Cl VB structures are not present in the ROHF determinant: delocalizing the SOMO on the $3p_x$ atomic orbitals of the chlorine atoms would realize a compromise that is very unfavourable energetically, then, the minimization of the energy imposes to sacrifice the $ClCu^+Cl^-$ and Cl^-Cu^+Cl VB structures to focus on the optimization of the orbitals for the $Cl^-Cu^{2+}Cl^-$ electronic distribution. There are many unpleasant consequences arising from this sacrifice, fully caused by the principle of energy minimization of a unique determinant. The first one is that the one body density matrix is qualitatively wrong using the ROHF wave function, which means that all the one body properties calculated with such an approach will also be qualitatively wrong. Moreover, the LMCT VB structure is energetically destabilized because it is described using the ROHF MO set. Finally, due to the fact that the $ClCu^+Cl^-$ and Cl^-Cu^+Cl VB structures are single excitations with respect to the ROHF determinant, they do not interact with the latter, they appear only at high order in PT (at least fourth order on the energy), and one has to include correctly the effect of the double excitations to bridge the interaction between them at the CI level. All the troubles of the post mean-field wave function methods to describe correctly the delocalization of the unpaired electron come from this critical unbalanced treatment of the two VB structures during the optimization of the orbitals in the mean-field treatment.

2. Performance of breathing orbital valence bond, orthogonal, and non-orthogonal

On the basis of the results of Sec. III D 1, one would like to perform a CI including all important VB structures, each one described with its own optimal orbitals. This would lead to a non-orthogonal CI recalling the breathing orbital Valence Bond (BOVB)[75] or the NOCI strategy.[4,5,9] Despite the complications due to the non-orthogonality of the molecular orbitals, such an approach is not directly related to the calculations previously reported. To tackle these problems, one can build the CI matrix between the ROHF and the $|\text{LMCT}\rangle_{opt}$ wave functions, which uses the ROHF orbitals as a common set of orthonormal orbitals (it is worth noticing that in this case the $|\text{LMCT}\rangle_{opt}$ wave function is a multideterminantal wave function). This can be seen as an orthogonal valence bond strategy[76–78] with breathing orbitals. One can easily find that the interaction between the $|\text{ROHF}\rangle$ and $|\text{LMCT}\rangle_{opt}$ is controlled by the double excitations that are single excitations on top of the $|\text{LMCT}\rangle$ determinant, just like in the intermediate Hamiltonian used in the previous paragraph. In this case, however, the c^{σ}_{pq} coefficients are fixed in order to have an optimal description of the LMCT structure (see Eq. (10)). We report in Figure 7 the values of the Hamiltonian matrix elements between the $|\text{LMCT}\rangle_{opt}$ and ROHF configurations, referred here as $H^{(breath)}$.

$$H^{(breath)} = \begin{array}{c} \\ \langle\text{ROHF}| \\ {}_{opt}\langle\text{LMCT}| \end{array} \begin{array}{c} \begin{array}{cc} |\text{ROHF}\rangle & |\text{LMCT}\rangle_{opt} \end{array} \\ \begin{pmatrix} 0.00 & 0.84 \\ 0.84 & 3.57 \end{pmatrix} \end{array}$$

FIG. 7. Hamiltonian matrix elements in the $|\text{ROHF}\rangle$ and $|\text{LMCT}\rangle_{opt}$ basis. ROHF orbitals are used, and values are reported in eV.

Despite the rather small stabilization of the ROHF effective energy caused by the $|\mu\rangle$'s which is introduced in $H^{(eff)}$ (see Figure 6), the $H^{(breath)}$ and $H^{(eff)}$ contain basically the same physical ingredients, and the main differences between them require some comments. In $H^{(eff)}$, the effect of the single excitations on top of the LMCT configuration is treated at second order in perturbation, whereas this effect is treated variationally in $H^{(breath)}$. The variational treatment gives a lower interaction (0.84 eV instead of 1.24 eV) together with a higher effective energy for the LMCT configuration (3.57 eV instead of 1.50 eV), implying that the single excitations on top of the LMCT configuration have a more tempered effect when one moves from perturbation to a variational treatment. Nevertheless, even at the strict variational level there is a lowering of the energy of the LMCT determinant of 7.58 eV, which is a remarkable effect. As said, the interaction between the LMCT configuration and some of its single excitations is as large as 7 eV, which clearly cannot be considered as a perturbation, explaining the failure of the perturbative $H^{(eff)}$ approach in the correct determination of the mixing between the ROHF and LMCT configuration.

The diagonalization of $H^{(breath)}$ can be seen as a contracted CI approach, and the lowest root of this Hamiltonian is referred hereafter to as $|\text{Contracted CI}\rangle$. If one releases the constraint imposed on the coefficients of the single excitations on top of $|\text{LMCT}\rangle$, it turns out to be a simple diagonalization of the CI matrix expressed in the basis of the $|\text{ROHF}\rangle$, $|\text{LMCT}\rangle$, and all the single excitations on top of $|\text{LMCT}\rangle$. This wave function is hereafter referred to as the uncontracted CI wave function ($|\text{Uncontracted CI}\rangle$). The global shape of $\Delta\rho(z)$ is reported in Figure 8 for the contracted and uncontracted wave functions, and compared to those obtained with ROHF and the largest CIPSI wave function.

From these figures, it appears that $\Delta\rho(z)$ obtained with the contracted and uncontracted wave functions are almost indistinguishable at this scale. Moreover, the global shape of the $\Delta\rho(z)$ for the contracted/uncontracted wave functions is close to that obtained with the near-FCI wave function. In

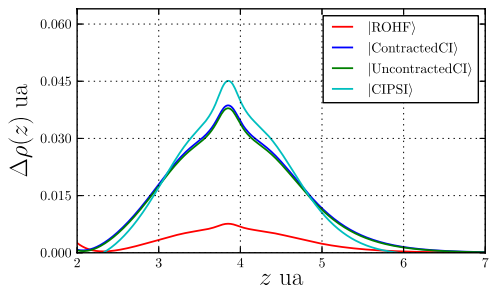

FIG. 8. $\Delta\rho(z)$ calculated with the contracted and uncontracted wave functions, compared with the CIPSI and ROHF $\Delta\rho(z)$ (see text).

the contracted/uncontracted wave function, the amplitude of the |LMCT⟩ determinant is about −0.197, which is very close to the value of −0.195 in the largest CIPSI wave function. These results confirm that the CI space here used contains all physical effects required for a correct description of the mixing between the ROHF and the LMCT determinants. To confirm this general point of view, non-orthogonal VB calculations have been performed using the XMVB-2.0 program.[79] In the 6-31G basis set, using the three VB structures ($ClCu^+Cl^-$, Cl^-Cu^+Cl, and $Cl^-Cu^{2+}Cl^-$) as the basic ingredients of the calculations, it appears that at the VB Self Consistent Field (VBSCF) the SD on the copper atom is 0.96, a value very close to 0.94 obtained at the ROHF level. The composition of the VBSCF wave function is dominated by the $Cl^-Cu^{2+}Cl^-$ VB structure, the $ClCu^+Cl^-$ and Cl^-Cu^+Cl VB structures having a negligible contribution. Moving to the BOVB approach, the SD on the copper atom is decreased to 0.86, a value which compares well with 0.87 obtained at near FCI level. In this case, the $ClCu^+Cl^-$ and Cl^-Cu^+Cl electronic structures bring considerable contributions to the wave function. On the other hand, the energy difference between the ground state and first excited state (essentially of LMCT character) passes from 11.07 eV at the VBSCF level, to 5.5 eV at the BOVB level, which is very similar to what has been obtained using the $|\text{LMCT}\rangle_{opt}$ and $H^{(breath)}$ approach.

E. Proposal of minimal CI space to compute accurately the spin density

As it has been highlighted in Secs. III A–III D, the delocalization of the unpaired electron is essentially given by the correct mixing of the ROHF and LMCT determinants. The wave function built with all single excitations with respect to these two determinants contains all physical ingredients required to obtain a SD of near-FCI quality. Such approach is referred to as the First-Order Breathing Orbital CI (FOBO-CI). The $\Delta\rho(z)$ calculated from the FOBO-CI wave function (|FOBO-CI⟩) built with the ROHF orbitals and with the natural orbitals of the |Contracted CI⟩ wave function is reported in Figure 9.

From this figure, it is apparent that the two $\Delta\rho(z)$ are very similar and very close to that computed with the largest CIPSI wave function, indicating that the FOBO-CI approach is quite stable with the change of the MO set. The fact that

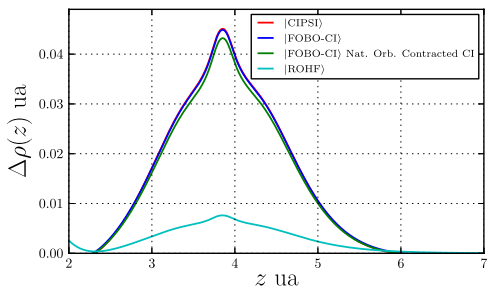

FIG. 9. $\Delta\rho(z)$ using the FOBO-CI approach, in the canonical MO set (|FOBO-CI⟩) and using the natural orbitals of the |Contracted CI⟩ wave function (|FOBO-CI⟩ Nat. Orb. Contracted CI). Comparison with the ROHF and largest CIPSI wave function.

the FOBO-CI approach gives such an accurate SD can be explained as follows. First, the FOBO-CI contains the two main determinants ruling the physics of the delocalization of the unpaired electron. Second, the FOBO-CI contains all the determinants that are single excitations on top of the two relevant configurations, which allows for the orbital relaxation of both configurations, and also bridge the interaction between them. Moreover, all the double excitations present in the FOBO-CI have in common the single excitation generating the LMCT configuration, which means that none of them are repeatable one after the other. This implies that disconnected terms in the FOBO-CI eigenvalue equation are absent and that this wave function is not subjected to size consistency errors, even if it remains a truncated CI. Finally, the FOBO-CI wave function contains also single excitations with respect to the ROHF determinant, which play different roles in this wave function. First, those determinants are double excitations with respect to the LMCT configuration and one can easily show that the bielectronic integrals involved in the interaction between the single excitations and the LMCT configuration are exactly the same involved in the interaction between the ROHF determinant and the double excitations present in the FOBO-CI wave function. This allows to have the same correlation effects for the ROHF determinant (with the double excitations) and for the LMCT configuration (with the single excitations with respect to the ROHF determinant). Second, the single excitations can introduce the spin polarization coming from the global distribution of the unpaired electrons, which is important for the correct determination of the SD. For all these reasons, the two main determinants are described in a very balanced way, which leads to a SD of near-FCI quality.

F. Effect of the basis set on the $\Delta\rho(z)$

The previous calculations have been performed using a modest basis set (6-31G) where the CIPSI algorithm can closely approach the FCI solution, thus giving reference values for the SD. Such an approach has allowed for the understanding of the key physical ingredients involved in the delocalization of the unpaired electron, and to propose the FOBO-CI strategy which has shown to reproduce very accurately the near-FCI shape of $\Delta\rho(z)$. Nevertheless, the obtained results must be considered as semi-quantitative because of the modest size of the 6-31G basis set, which lacks diffuse and polarization functions, for instance. Here, the FOBO-CI is used as a tool to study the effect of the basis set on the global shape of $\Delta\rho(z)$, considering basis sets for which the CIPSI algorithm would need an excessively large number of determinants to reach convergence. The $\Delta\rho(z)$ has been computed with the FOBO-CI and ROHF wave functions with three types of basis sets of double and triple zeta quality: the correlation consistent basis set (cc-pVDZ, cc-pVTZ), the same basis set augmented with diffuse functions (aug-cc-pVDZ, aug-cc-pVTZ),[80,81] and the Roos augmented atomic natural orbitals[82,83] (ANO-DZ, ANO-TZ). For the sake of clarity, only the results obtained for the cc-pVXZ, ANO-XZ (X = D,T), and 6-31G are shown in Figure 10. From this figure, it appears that at the ROHF level, the global shape of $\Delta\rho(z)$ is unchanged moving from the 6-31G to the ANO-DZ basis sets. The same behaviour is also observed

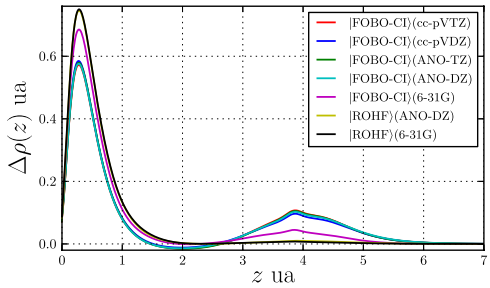

FIG. 10. $\Delta\rho(z)$ using the FOBO-CI and ROHF wave function in various basis sets.

for the other basis sets, suggesting that the optimal orbitals for the $Cl^-Cu^{2+}Cl^-$ VB structure depend weakly on the basis set. Using the FOBO-CI wave function, three main qualitative differences can be observed moving from the 6-31G to the cc-pVXZ, aug-cc-pVXZ, and ANO-XZ (X = D,T) basis sets. First, the SD is much higher on the chlorine ligands using the cc-pVXZ, aug-cc-pVXZ, and ANO-XZ basis sets. This can be understood considering that the SD on the chlorine atoms is originated from the correct relaxation of the two $ClCu^+Cl^-$ and Cl^-Cu^+Cl VB structures which requires flexibility, especially on the copper atom. Second, using the cc-pVXZ, aug-cc-pVXZ, and ANO-XZ basis sets the shape of the $\Delta\rho(z)$ is no longer spherical around the chlorine ligands. This behaviour is due to the polarization functions on the chlorine ligands which allow the singly occupied $3p_x$ orbitals of the $ClCu^+Cl^-$ and Cl^-Cu^+Cl VB structures to be distorted towards the "outside" of the molecule, in order to avoid the increased electronic density on the Cu^+ center. Third, a notable negative SD appears between the Cu and the Cl atoms, suggesting that the spin polarization mechanism is important here. Finally, the global shape of $\Delta\rho(z)$ using the four basis sets having polarization functions is almost indistinguishable. To obtain a quantity summarizing the information of the $\Delta\rho(z)$ in one number, the SD on the copper atom has been calculated with the MPA approach on the ROHF and the FOBO-CI wave functions for all basis sets. The results, together with those obtained with DFT (B3LYP functional), are reported in Table III. From this table, it appears that, for a given WFT model, the SD on the copper atom weakly depends on the basis set as soon as polarization and diffuse functions are included. Moreover, a strong reduction of the SD on the Cu atom is confirmed moving from the self consistent field model to a fully correlated approach, thus supporting the interpretative schemes in which the SCF approach strongly penalizes the VB structures with the unpaired electron on the Cl atoms. Such a biased description is corrected improving the representation of these structures by allowing the orbitals to relax and to be optimal also for these charge distributions. As the FOBO-CI has shown to reproduce very accurately the $\Delta\rho(z)$ at near-FCI level with the 6-31G basis set, it is reasonable to propose a value of 0.68(1) unpaired electrons on the copper atom at the non-relativistic FCI level using a basis set of augmented triple zeta quality with polarization functions.

TABLE III. Values of the spin density on the copper atom using MPA with the ROHF and FOBO-CI wave functions in various basis sets. DFT (B3LYP) values are reported for comparison.

Basis set	SD (Cu) ROHF	SD (Cu) FOBO-CI	B3LYP
6-31G	0.942	0.880	0.703
cc-pVDZ	0.970	0.685	0.496
cc-pVTZ	0.970	0.665	0.495
aug-cc-pVDZ	0.971	0.675	0.511
aug-cc-pVTZ	0.971	0.680	0.499
ANO-DZ	0.970	0.672	...
ANO-TZ	0.971	0.688	...

IV. APPLICATION TO $[CuCl_4]^{2-}$

The Cu atom in this system is in a $3d^9$ configuration. The ground state is a doublet and the SOMO belongs to the b_{1g} irreducible representation of the D_{4h} symmetry group of the molecule. The chlorine atoms are placed on the x and y axes and the Cu–Cl distance is taken to be 2.291 Å which is the optimal CASPT2 value computed by Pierloot and Vancoillie.[21] At the mean-field level, both single and multiconfigurational, the SOMO is dominated by the $3d_{x^2-y^2}$ Cu atomic orbital with small contributions of the chlorine $3p_x$ and $3p_y$ orbitals pointing toward the Cu atom. This results in a SD on the copper atom at mean-field level which is between 0.92 and 0.84, as it has been found in previous studies,[20,21] too high a value if compared to the experimental finding of 0.62(2). This overestimation of the SD on the copper atom indicates that the mean-field methods underestimate the delocalization of the unpaired electron between the copper and chlorine atoms, resulting in a too ionic Cu–Cl bond, just like in the $CuCl_2$ molecule. In order to apply the FOBO-CI method, one has to identify the LMCT determinant responsible for the delocalization of the unpaired electron, that is, a single excitation from a b_{1g} orbital (dominated by contributions of the AOs belonging to the chlorine ligands) to the SOMO. Intuitively, the molecular orbital obtained from the combination (with the proper phase) of the $3p_x$ and $3p_y$ AOs of the chlorine ligands pointing to the Cu atom is a good candidate. The FOBO-CI consists of the diagonalization of the CI matrix built with all single excitations with respect to the ROHF and the appropriate LMCT determinants. The results for the SD (computed with the MPA) on the copper atom for the ROHF and FOBO-CI wave functions are reported in Table IV for various basis sets and compared

TABLE IV. Values of the spin density on the copper atom using MPA with the ROHF and FOBO-CI wave functions and various basis sets, compared with DFT (B3LYP) and the experimental value.

Basis set	SD (Cu) ROHF	SD (Cu) FOBO-CI	B3LYP
6-31G	0.93	0.81	0.70
cc-pVDZ	0.92	0.63	0.55
cc-pVTZ	0.92	0.66	0.55
ANO-DZ	0.92	0.65	...
Experimental SD (Cu)[24,25]			
0.62(2)			

to the SD obtained with DFT using the B3LYP functional. From this table, it appears that the FOBO-CI spin density is quite stable with respect to the basis set, as soon as the basis set is of good quality. Moreover, the FOBO-CI wave function gives SD values between 0.63 and 0.66, a range very close to the experimental finding of 0.62(2). In the FOBO-CI wave function obtained with the ANO-DZ basis set, the determinant having largest coefficient, besides the ROHF determinant, is the LMCT determinant whose amplitude is about 0.25, which is unusual for a single excitation. The LMCT determinant is 12.65 eV higher in energy than the ROHF determinant, but if one performs the contracted CI previously described (see Eq. (10)) of the LMCT and its own single excitations (in order to relax the orbitals of the LMCT configuration) the energy difference decreases to 5.11 eV. This behavior is very similar to that observed for $CuCl_2$: the dominant configuration after the ROHF determinant is a single excitation and the relaxation of the orbitals on such determinant has a huge energetic impact. If one uses the natural orbitals of the FOBO-CI wave function to build a pseudo Hartree-Fock determinant, one obtains a SD on the copper atom of about 0.72, which is not in perfect agreement with the experimental value but represents an important improvement with respect to all mean-field approaches reported for this system. It should be pointed out that the DFT results underestimate the SD on the copper atom if polarization functions are used, implying that such an approach overestimates the importance of the LMCT VB structures, a reasonable result if one considers that DFT tends to underestimate the energy of the charge transfer states. Similar results have also been observed by Szilagyi *et al.* with the BP86 functional.[34]

V. CONCLUSION AND DISCUSSIONS

In this work, the $CuCl_2$ and $[CuCl_4]^{2-}$ molecules have been considered as prototypes to investigate the physics of the metal-ligand delocalization through a detailed study of the SD. The main computational tools used here belong to WFT. Every approach has provided a clue to understand the various problems encountered using WFT for these systems. One can summarize the main ingredients leading to a good description for these systems as follows. First, there are two types of VB structures that dominate the fully correlated wave function and the correct metal-ligand delocalization is controlled by the proper mixing between these two types of VB structures. The most important VB structure is the one where the copper atom is in its $Cu^{2+}(3d^9)$ oxidation state and the chlorine ligands in the $Cl^-(3p^6)$ state. The other important VB structures represent the resonance of all electronic distributions where the copper atom is in its $Cu^+(3d^{10})$ ionized form and one chlorine atom in its neutral form, the other remaining ligands being Cl^-. All VB structures belonging to this class can be considered as charge transfer states where an electron is excited from one ligand to the metal, thus, all are single excitations with respect to the dominant VB form. Using symmetry adapted molecular orbitals (as it is the case here), all these VB structures can be taken into account with a unique single excitation, the LMCT configuration, where a β electron is promoted from a doubly occupied molecular orbital belonging to the same irreducible representation as the SOMO and dominated by the appropriate $3p$ chlorine atomic orbitals. The use of mean-field optimization procedures, both single and multireference, provide optimal orbitals for the dominant VB structure, which markedly penalize the LMCT structure, shifting its energy at too high a value, thus such approaches miss, almost totally, the LMCT VB structure. As it has been shown, the two types of dominant VB structures are energetically very sensitive to the MOs and they need different types of optimal MOs. This requirement cannot be taken into account at the mean-field level, which explains why only the more stable of the two VB structures is present in the mean-field wave functions. It should be mentioned that this kind of problem occurs also at the SCF level in other applications, such as in bond length alternation in conjugated pi systems,[84,85] or in the determination of correctly delocalized molecular orbitals in organic magnetic molecules,[86,87] where in any case, neutral and ionic components of the wave function cannot be both correctly treated using a mean-field approach. To correct this biased treatment, one has to include the double excitations on top of the mean-field wave function using a size consistent approach in order to realize properly a bridging interaction between the two dominant classes of VB structures. Among the double excitations, those who are single excitations on top of the LMCT configuration have shown to play a crucial role, as they strongly relax the orbitals of the LMCT configuration. This has been found to be compulsory to allow for the correct mixing between the various VB structures in the ground state wave function. Similar considerations have been reported previously in pioneering works in this field,[5,9] for other transition metal containing systems. The orbital relaxation of the various VB structures has been considered in such studies within a non-orthogonal CI approach. The understanding of the key ingredients of the problem has led us to a proposal of a minimal CI space (the FOBO-CI approach) which stays within an orthogonal CI strategy, fulfilling all conditions found here to allow for the correct determination for the SD in such systems. It contains the dominant VB structures and all determinants required to relax their own orbitals, it also contains the determinants describing the spin polarization, it is free from size consistency errors, and it introduces electronic correlation in a very balanced way between the various VB structures. The FOBO-CI approach has shown, at a reasonable computation cost, to reproduce accurately the SD on the copper atom, both for the $CuCl_2$ and the $[CuCl_4]^{2-}$ ground states. For the $CuCl_2$ molecule, near-FCI reference values have been obtained in the modest 6-31G basis set using the CIPSI algorithm and the FOBO-CI has shown to reproduce very accurately these results. For $[CuCl_4]^{2-}$, the SD obtained with the FOBO-CI approach is in very good agreement with the available experimental data. On the basis of such successes, a reference value for the SD on the copper atom in $CuCl_2$ (non-relativistic, near-FCI, and extended basis sets), for which experimental values are not available, has been proposed.

It should be pointed out that the FOBO-CI approach contains the LMCT configuration and its single excitations, which can be interpreted as determinants belonging to the $1h$ and $2h1p$ classes of excitations, respectively. The simultaneous presence of such excitation classes was identified as crucial

for the metal-ligand delocalization in binuclear complexes in Refs. 7, 8, and 10. In such works, the $2h1p$ excitations were found to increase the weight of the $1h$ LMCT determinants and this increase was interpreted as a correlation induced delocalization of the magnetic orbitals, with respect to the minimal CASSCF(2,2) orbitals. Using the $CuCl_2$ and $[CuCl_4]^{2-}$ as prototypes of transition metal containing systems, it has been shown that this delocalization is a purely static effect given that among the $2h1p$ excitations, the most important are those describing the relaxation of the orbitals of the LMCT determinant, which are different from the optimal orbitals of the dominant VB structure (unpaired electron on the Cu atom). This electronic structures are artificially removed from the mean-field wave function by the orbital optimization procedure. Such a biased description, which leads to an excessive localization of the unpaired electron on the Cu atom, is at the origin of the difficulties previously observed in the calculation the spin density. Indeed, the orbital relaxation, if not described within an *ad hoc* strategy, is taken into account only at high level of theory (in PT at least second order on the wave function and variational logic at DDCI2 or very large selected CI space). The FOBO-CI strategy, here proposed, staying within a scheme based on a unique set of MOs, aims at mimicking the individual orbital optimization for the two relevant VB structures. Because the FOBO-CI relies on the identification of the meaningful LMCT determinants, further work in progress will focus our attention on the systematic determination of these determinants.

[1]S. Petit, S. A. Borshch, and V. Robert, "*Ab initio* simulation of paramagnetic NMR spectra: The ^{31}P NMR in oxovanadium phosphates," J. Am. Chem. Soc. **125**, 3959–3966 (2003).

[2]M. A. Aebersold, B. Gillon, O. Plantevin, L. Pardi, O. Kahn, P. Bergerat, I. von Seggern, F. Tuczek, L. Öhrström, A. Grand, and E. Lelièvre-Berna, J. Am. Chem. Soc. **120**, 5238–5245 (1998).

[3]J. A. Aramburu and M. Moreno, "Bonding in d^9 complexes derived from EPR: Application to $cucl^2$, $cubr^2$, and $cdcl_2$:cu^{2+}," J. Chem. Phys. **83**, 6071–6083 (1985).

[4]G. J. M. Janssen and W. C. Nieuwpoort, "Band gap in Nio: A cluster study," Phys. Rev. B **38**, 3449–3458 (1988).

[5]A. van Oosten, R. Broer, and W. Nieuwpoort, "Heisenberg exchange enhancement by orbital relaxation in cuprate compounds," Chem. Phys. Lett. **257**, 207–212 (1996).

[6]C. J. Calzado, J. Cabrero, J. P. Malrieu, and R. Caballol, "Analysis of the magnetic coupling in binuclear complexes. I. Physics of the coupling," J. Chem. Phys. **116**, 2728–2747 (2002).

[7]C. J. Calzado, J. F. Sanz, and J. P. Malrieu, "Accurate *ab initio* determination of magnetic interactions and hopping integrals in $La_{2-x}Sr_xCuO_4$ systems," J. Chem. Phys. **112**, 5158–5167 (2000).

[8]J. Cabrero, C. J. Calzado, D. Maynau, R. Caballol, and J. P. Malrieu, "Metal ligand delocalization in magnetic orbitals of binuclear complexes," J. Phys. Chem. A **106**, 8146–8155 (2002).

[9]R. Broer, L. Hozoi, and W. C. Nieuwpoort, "Non-orthogonal approaches to the study of magnetic interactions," Mol. Phys. **101**, 233–240 (2003).

[10]C. J. Calzado, C. Angeli, D. Taratiel, R. Caballol, and J.-P. Malrieu, "Analysis of the magnetic coupling in binuclear systems. III. The role of the ligand to metal charge transfer excitations revisited," J. Chem. Phys. **131**, 044327 (2009).

[11]C. de Graaf, C. Sousa, I. d. P. R. Moreira, and F. Illas, J. Phys. Chem. A **105**, 11371–11378 (2001).

[12]M. Spivak, C. Angeli, C. J. Calzado, and C. de Graaf, "Improving the calculation of magnetic coupling constants in MRPT methods," J. Comput. Chem. **35**, 1665–1671 (2014).

[13]C. Angeli and C. J. Calzado, "The role of the magnetic orbitals in the calculation of the magnetic coupling constants from multireference perturbation theory methods," J. Chem. Phys. **137**, 034104 (2012).

[14]C. Angeli, R. Cimiraglia, S. Evangelisti, T. Leininger, and J.-P. Malrieu, "Introduction of n electron valence states for multireference perturbation theory," J. Chem. Phys. **114**, 10252–10264 (2001).

[15]C. Angeli, R. Cimiraglia, and J. P. Malrieu, "N electron valence state perturbation theory: A fast implementation of the strongly contracted variant," Chem. Phys. Lett. **350**, 297–305 (2001).

[16]C. Angeli, R. Cimiraglia, and J. P. Malrieu, "N electron valence state perturbation theory: A spinless formulation and an efficient implementation of the strongly contracted and of the partially contracted variants," J. Chem. Phys. **117**, 9138–9153 (2002).

[17]K. Andersson, P. A. Malmqvist, B. O. Roos, A. J. Sadlej, and K. Wolinski, "Second-order perturbation theory with a CASSCF reference function," J. Phys. Chem. **94**, 5483–5488 (1990).

[18]J. Miralles, O. Castell, R. Caballol, and J.-P. Malrieu, "Specific CI calculation of energy differences: Transition energies and bond energies," Chem. Phys. **172**, 33–43 (1993).

[19]F. Neese, "Sum-over-states based multireference *ab initio* calculation of EPR spin Hamiltonian parameters for transition metal complexes. A case study," Magn. Reson. Chem. **42**, S187–S198 (2004).

[20]S. Vancoillie, P.-A. Malmqvist, and K. Pierloot, "Calculation of EPR g tensors for transition-metal complexes based on multiconfigurational perturbation theory (CASPT2)," ChemPhysChem **8**, 1803–1815 (2007).

[21]S. Vancoillie and K. Pierloot, J. Phys. Chem. A **112**, 4011–4019 (2008).

[22]M. M. Francl, W. J. Pietro, W. J. Hehre, J. S. Binkley, M. S. Gordon, D. J. DeFrees, and J. A. Pople, "Self consistent molecular orbital methods. XXIII. A polarization type basis set for second row elements," J. Chem. Phys. **77**, 3654–3665 (1982).

[23]V. A. Rassolov, J. A. Pople, M. A. Ratner, and T. L. Windus, "6-31G* basis set for atoms k through Zn," J. Chem. Phys. **109**, 1223–1229 (1998).

[24]A. A. Gewirth, S. L. Cohen, H. J. Schugar, and E. I. Solomon, "Spectroscopic and theoretical studies of the unusual EPR parameters of distorted tetrahedral cupric sites: Correlations to x-ray spectral features of core levels," Inorg. Chem. **26**, 1133–1146 (1987).

[25]S. V. Didziulis, S. L. Cohen, A. A. Gewirth, and E. I. Solomon, "Variable photon energy photoelectron spectroscopic studies of copper chlorides: An experimental probe of metal-ligand bonding and changes in electronic structure on ionization," J. Am. Chem. Soc. **110**, 250–268 (1988).

[26]A. Ramírez-Solís, R. Poteau, A. Vela, and J. P. Daudey, "Comparative studies of the spectroscopy of $cucl_2$: DFT versus standard *ab initio* approaches," J. Chem. Phys. **122**, 164306 (2005).

[27]M. Caffarel, E. Giner, A. Scemama, and A. Ramírez-Solís, "Spin density distribution in open-shell transition metal systems: A comparative post-Hartree–Fock, density functional theory, and quantum Monte Carlo study of the $CuCl_2$ molecule," J. Chem. Theory Comput. **10**, 5286 (2014).

[28]R. S. Mulliken, "Electronic population analysis on lCAOo–MO molecular wave functions. I," J. Chem. Phys. **23**, 1833–1840 (1955).

[29]V. N. Staroverov, G. E. Scuseria, J. Tao, and J. P. Perdew, "Comparative assessment of a new nonempirical density functional: Molecules and hydrogen-bonded complexes," J. Chem. Phys. **119**, 12129–12137 (2003).

[30]Y. Zhao and D. Truhlar, "The M06 suite of density functionals for main group thermochemistry, thermochemical kinetics, noncovalent interactions, excited states, and transition elements: Two new functionals and systematic testing of four M06-class functionals and 12 other functionals," Theor. Chem. Acc. **120**, 215–241 (2008).

[31]C. Lee, W. Yang, and R. G. Parr, "Development of the colle salvetti correlation energy formula into a functional of the electron density," Phys. Rev. B **37**, 785–789 (1988).

[32]A. D. Becke, "Density functional thermochemistry. III. The role of exact exchange," J. Chem. Phys. **98**, 5648–5652 (1993).

[33]A. D. Becke, "Density-functional exchange-energy approximation with correct asymptotic behavior," Phys. Rev. A **38**, 3098–3100 (1988).

[34]R. K. Szilagyi, M. Metz, and E. I. Solomon, "Spectroscopic calibration of modern density functional methods using $[CuCl_4]^{2-}$," J. Phys. Chem. A **106**, 2994–3007 (2002).

[35]E. Ruiz, J. Cano, S. Alvarez, and P. Alemany, "Magnetic coupling in end-on azido-bridged transition metal complexes, a density functional study," J. Am. Chem. Soc. **120**, 11122–11129 (1998).

[36]M. Atanasov, P. Comba, B. Martin, V. Müller, G. Rajaraman, H. Rohwer, and S. Wunderlich, "DFT models for copper(ii) bispidine complexes: Structures, stabilities, isomerism, spin distribution, and spectroscopy," J. Comput. Chem. **27**, 1263–1277 (2006).

[37]B. Huron, P. Rancurel, and J. Malrieu, J. Chem. Phys. **58**, 5745 (1973).

[38]S. Evangelisti, J. Daudey, and J. Malrieu, Chem. Phys. **75**, 91 (1983).

[39]A. D. Becke, "Basis-set-free density-functional quantum chemistry," Int. J. Quantum Chem. **36**, 599–609 (1989).

[40]J. P. Perdew, "Density-functional approximation for the correlation energy of the inhomogeneous electron gas," Phys. Rev. B **33**, 8822–8824 (1986).
[41]C. Remenyi, R. Reviakine, and M. Kaupp, "Density functional study of EPR parameters and spin-density distribution of azurin and other blue copper proteins," J. Phys. Chem. B **111**, 8290–8304 (2007).
[42]E. Bosch, P. Crozet, A. Ross, and J. Brown, "Fourier transform spectra of the $E^2\Pi_u$–$X^2\Pi_{g(3/2)}$ system of $cucl_2$: 2. Rovibronic levels of the ground state up to 4000 cm:1," J. Mol. Spectrosc. **202**, 253–261 (2000).
[43]J.-P. Daudey, J.-L. Heully, and J.-P. Malrieu, "Size consistent self consistent truncated or selected configuration interaction," J. Chem. Phys. **99**, 1240–1254 (1993).
[44]J. Meller, J. L. Heully, and J. P. Malrieu, "Size-consistent self-consistent combination of selected CI and perturbation theory," Chem. Phys. Lett. **218**, 276–282 (1994).
[45]J. P. Malrieu, J. P. Daudey, and R. Caballol, "Multireference self consistent size consistent singles and doubles configuration interaction for ground and excited states," J. Chem. Phys. **101**, 8908–8921 (1994).
[46]C. F. Bender and E. R. Davidson, Phys. Rev. **183**, 23 (1969).
[47]R. J. Buenker and S. D. Peyerimhoff, Theor. Chim. Acta **35**, 33 (1974).
[48]R. J. Buenker, S. D. Peyerimhoff, and P. J. Bruna, *Computational Theoretical Organic Chemistry* (Reidel, Dordrecht, 1981), p. 55.
[49]R. J. Harrison, J. Chem. Phys. **94**, 5021 (1991).
[50]J. Rubio, J. Novoa, and F. Illas, "Convergence of a multireference second-order mbpt method (CIPSI) using a zero-order wavefunction derived from an {MS}{SCF} calculation," Chem. Phys. Lett. **126**, 98–102 (1986).
[51]R. Cimiraglia and M. Persico, "Recent advances in multireference second order perturbation CI: The CIPSI method revisited," J. Comput. Chem. **8**, 39–47 (1987).
[52]C. Angeli and M. Persico, "Multireference perturbation CI II. Selection of the zero-order space," Theor. Chem. Acc. **98**, 117–128 (1997).
[53]C. Angeli, R. Cimiraglia, and J.-P. Malrieu, "On a mixed Møller–Plesset Epstein–Nesbet partition of the Hamiltonian to be used in multireference perturbation configuration interaction," Chem. Phys. Lett. **317**, 472–480 (2000).
[54]G. Emmanuel, S. Anthony, and C. Michel, "Using perturbatively selected configuration interaction in quantum Monte Carlo calculations," Can. J. Chem. **91**, 879–885 (2013).
[55]A. Scemama, T. Applencourt, E. Giner, and M. Caffarel, "Accurate nonrelativistic ground-state energies of 3d transition metal atoms," J. Chem. Phys. **141**, 244110 (2014).
[56]E. Giner, A. Scemama, and M. Caffarel, "Fixed-node diffusion Monte Carlo potential energy curve of the fluorine molecule f_2 using selected configuration interaction trial wavefunctions," J. Chem. Phys. **142**, 044115 (2015).
[57]F. A. Evangelista, "Adaptive multiconfigurational wave functions," J. Chem. Phys. **140**, 124114 (2014).
[58]P. S. Epstein, "The stark effect from the point of view of Schroedinger's quantum theory," Phys. Rev. **28**, 695–710 (1926).
[59]R. K. Nesbet, "Configuration interaction in orbital theories," Proc. R. Soc. London, Ser. A **230**, 312–321 (1955).
[60]C. Angeli and R. Cimiraglia, "Multireference perturbation CI IV. Selection procedure for one electron properties," Theor. Chem. Acc. **105**, 259–264 (2001).
[61]M. S. Gordon and M. W. Schmidt, "Advances in electronic structure theory: GAMESS a decade later," in *Theory and Applications of Computational Chemistry: The First Forty Years*, edited by C. E. Dykstra, G. Frenking, K. S. Kim, and G. E. Scuseria (Elsevier, Amsterdam, 2005), pp. 1167–1189.
[62]A. Scemama, E. Giner, T. Applencourt, G. David, and M. Caffarel, Quantum package v0.6, Zenodo, 2015, available at https://zenodo.org/record/30304#.VgGW75fO5h5.
[63]L. Brillouin, "Le champ self-consistent, pour des électrons liés; la supraconductibilité," J. Phys. Radium **4**, 333–361 (1933).
[64]B. Levy and G. Berthier, "Generalized brillouin theorem for multiconfigurational SCF theories," Int. J. Quantum Chem. **2**, 307–319 (1968).
[65]J. A. Pople, M. Head Gordon, and K. Raghavachari, "Quadratic configuration interaction. A general technique for determining electron correlation energies," J. Chem. Phys. **87**, 5968–5975 (1987).
[66]J. Goldstone, "Derivation of the brueckner many-body theory," Proc. R. Soc. London, Ser. A **239**, 267–279 (1957).
[67]I. Nebot Gil, J. Sanchez Marin, J. P. Malrieu, J. L. Heully, and D. Maynau, "Self consistent intermediate Hamiltonians: A coupled cluster type formulation of the singles and doubles configuration interaction matrix dressing," J. Chem. Phys. **103**, 2576–2588 (1995).
[68]J. P. Malrieu, P. Durand, and J. P. Daudey, "Intermediate Hamiltonians as a new class of effective Hamiltonians," J. Phys. A: Math. Gen. **18**, 809 (1985).
[69]J. P. Malrieu, J. L. Heully, and A. Zaitsevskii, "Multiconfigurational second order perturbative methods: Overview and comparison of basic properties," Theor. Chim. Acta **90**, 167–187 (1995).
[70]J. L. Heully, J. P. Malrieu, and A. Zaitsevskii, "On the origin of size inconsistency of the second order state specific effective Hamiltonian method," J. Chem. Phys. **105**, 6887–6891 (1996).
[71]Note that similar integrals appear in the Fock operator of the Cu^+ cation described with Cu^{2+} ROHF orbitals.
[72]H. F. King, R. E. Stanton, H. Kim, R. E. Wyatt, and R. G. Parr, "Corresponding orbitals and the nonorthogonality problem in molecular quantum mechanics," J. Chem. Phys. **47**, 1936–1941 (1967).
[73]A. Domingo, C. Angeli, C. de Graaf, and V. Robert, "Electronic reorganization triggered by electron transfer: The intervalence charge transfer of a fe^{3+}/fe^{2+} bimetallic complex," J. Comput. Chem. **36**, 861–869 (2015).
[74]B. Meyer, A. Domingo, T. Krah, and V. Robert, "Charge transfer processes: The role of optimized molecular orbitals," Dalton Trans. **43**, 11209–11215 (2014).
[75]P. C. Hiberty and S. Shaik, "Breathing-orbital valence bond method, a modern valence bond method that includes dynamic correlation," Theor. Chem. Acc. **108**, 255–272 (2002).
[76]J.-P. Malrieu, N. Guihéry, C. j. Calzado, and C. Angeli, "Bond electron pair: Its relevance and analysis from the quantum chemistry point of view," J. Comput. Chem. **28**, 35–50 (2007).
[77]J. P. Malrieu, C. Angeli, and R. Cimiraglia, "On the relative merits of non orthogonal and orthogonal valence bond methods illustrated on the hydrogen molecule," J. Chem. Educ. **85**, 150 (2008).
[78]A. F. Sax, "Chemical bonding: The orthogonal valence-bond view," Int. J. Mol. Sci. **16**, 8896–8933 (2015).
[79]Z. Chen, F. Ying, X. Chen, J. Song, P. Su, L. Song, Y. Mo, Q. Zhang, and W. Wu, "Xmvb 2.0: A new version of xiamen valence bond program," Int. J. Quantum Chem. **115**, 731–737 (2015).
[80]D. E. Woon and T. H. Dunning, "Gaussian basis sets for use in correlated molecular calculations. III. The atoms aluminum through argon," J. Chem. Phys. **98**, 1358–1371 (1993).
[81]N. B. Balabanov and K. A. Peterson, "Systematically convergent basis sets for transition metals. I. All-electron correlation consistent basis sets for the 3d elements sc–zn," J. Chem. Phys. **123**, 064107 (2005).
[82]J. Bauschlicher and W. Charles, "Large atomic natural orbital basis sets for the first transition row atoms," Theor. Chim. Acta **92**, 183–198 (1995).
[83]P. O. Widmark, B. Persson, and B. Roos, "Density matrix averaged atomic natural orbital (ano) basis sets for correlated molecular wave functions," Theor. Chim. Acta **79**, 419–432 (1991).
[84]W. T. Borden and E. R. Davidson, "Theoretical studies of diradicals containing four .pi. Electrons," Acc. Chem. Res. **14**, 69–76 (1981).
[85]W. T. Borden, E. R. Davidson, and D. Feller, "Rhf and two-configuration scf calculations are inappropriate for conjugated diradicals," Tetrahedron **38**, 737–739 (1982).
[86]N. Suaud, R. Ruamps, N. Guihéry, and J. P. Malrieu, "A strategy to determine appropriate active orbitals and accurate magnetic couplings in organic magnetic systems," J. Chem. Theory Comput. **8**, 4127–4137 (2012).
[87]N. Suaud, R. Ruamps, J. P. Malrieu, and N. Guihéry, J. Phys. Chem. A **118**, 5876–5884 (2014).